CIVIL ENGINEERING JOURNAL

Article no. 37

THE CIVIL ENGINEERING JOURNAL 4-2023

MECHANICAL CHARACTERISTICS OF LARGE-SECTION TUNNEL IN SOFT ROCK BASED ON VARIOUS ROCK CONDITIONS AND EXCAVATION FOOTAGES

Zengyin Xia[1], Chi Zhang[2], Pan Cao[3], Bin Li[2], Gongning Liu[3] and Huijian Zhang[3]

1. *China Railway Tunnel Group Road & Bridge Engineering Co.，Ld.，Tianjin 30030 China*
2. *China Railway Design Corporation, Tianjin 300308, China*
3. *Southwest Jiaotong University, Key Laboratory of Transportation Tunnel Engineering, Ministry of Education, Chengdu, No. 111, North Section, Second Ring Road, Jinniu District, 610031, China; 305434884@qq.com; 2995484603@qq.com; huijianz@163.com*

ABSTRACT

At present, few studies have taken both the rock conditions and the excavation footages into account to study the mechanical and deformation characteristics of the tunnel in soft rock area, and the existing results cannot be simply applied. Therefore, taking the Qianqi tunnel in V-class surrounding rock area as an example, based on the numerical calculation method, the mechanics and deformation rules about the tunnel under various rock conditions as well as excavation footages are analyzed in detail, aiming to provide some vital references for the on-site construction of the relied tunnel project. The results show that the displacements of the surrounding rock are greatly influenced by the excavation footages, namely, the arch settlements, horizontal convergences of the tunnel as well as the surface settlement increase significantly with the excavation footages. For the competent rock condition, the maximum bending moments of the preliminary lining after excavation occurs in the vault, and its increase amplitude has little correlation with the excavation footage that is more than 1.5m. For the poor surrounding rock, the maximum bending moment is transferred from the vault to the arch waist with the increase of the excavation footage, and it is basically manifested as the inner tension of the lining. The relationship between the excavation footage and maximum deformation as well as the mechanical index of the vault is also revealed, respectively. The excavation footage of the relied tunnel project is suggested as follows: 1.8m and 1.2m for the competent and poor rock conditions, respectively.

KEYWORD

Excavation footage, Soft rock, Three-bench method, Shallow-buried tunnel, mechanical property

INTRODUCTION

The stability of tunnel is always the focus of research [1, 2], especially for the tunnel in the weak surrounding rock [3, 4], and its stability is also closely related to construction method. According

to domestic and foreign engineering experience, if the full-section excavation method is not suitable for tunnels, bench method is often used [5]. As one of the main methods of mine tunnel construction, the bench method is essentially a geologically oriented excavation method [6]. With the change of surrounding rock conditions, the length of steps, the number and size of divided sections can also be changed accordingly, and the method is flexible in form, featuring fewer excavation disturbance of surrounding rock, favorable control of surrounding rock deformation and timely lining [7-10]. However, when the bench method is used in construction, there is no clear standard for the excavation footage, and the existing research results cannot be simply applied. If the excavation footage is set too small, it will prolong the excavation period as well as increase the construction cost. If the excavation footage is too large, when the rocks is poor, the stabilities of the surrounding rock at the tunnel vault as well as the excavation face will be particularly prominent, which is extremely unfavorable to the safety of the tunnel, and may even cause collapse in serious cases [11-17].

Scholars pointed out that the large deformation of tunnel excavation face could be effectively controlled by using the three-bench temporary invert method and reinforcing the upper step with the fibreglass bolts [18]. Within a certain range, the spacing of up and down steps of the tunnel, the spacing of annular and longitudinal bolts are negatively correlated with the stabilities of tunnel, and the parameters should be adjusted according to the actual situation [19]. The construction disturbance of super-large section tunnel is mainly concentrated in the excavation stage of the soil of upper step [20]. Using the bench method, the deformation properties about the tunnel during construction with freezing pipe roof was analyzed, and it was found that the demolition of temporary linings had a great effect on the displacement as well as the force of the tunnel, and the force centralization about the linings was alleviated after thawing [21]. The formation settlement properties about the tunnel in loess were analyzed, and it was found that the upper strata of the tunnel area sank as a whole after excavation, which developed rapidly and was destructive [22].

As can be seen from the previous studies, although many researches have been carried out on the construction of tunnel using the bench method, while few studies have comprehensively considered both the rock conditions and excavation footages. At the same time, due to the differences in engineering geological conditions (including the parameters of surrounding rock and lining, high in-situ stress, buried depth, etc.) of the tunnels in different studies [23, 24], the existing results cannot be simply applied to the relied project of this paper, and further studies should be carried out based on specific projects to provide more targeted construction suggestions.

Based on the two engineering examples of Qianqi Tunnel with similar excavation depth, similar strata and different water content, the deformation rules as well as the mechanics about the tunnel in various excavation footages for these two conditions are compared by numerical calculation, and the reasonable excavation footage of tunnel in V-grade soft rock is also proposed accordingly, aiming to provide relevant reference for the construction and design about similar project.

ENGINEERING BACKGROUND

Qianqi Tunnel locates in Ulanqab City, Inner Mongolia Autonomous region. It is a high-speed railway tunnel with a starting as well as ending mileage of DK32+380 ~ DK36+649. The total length and maximum buried depth about the tunnel are 4,269 m and 141 m, respectively. The total length

of the V- grade rock section about the whole tunnel is 2349 m, occupying 55.03% of the whole length. The plan view and cross-section map of tunnel is shown in Figure 1. The tunnel span and height are 14.96m and 13.14m, respectively. According to the geological data, the entrance as well as the exit section about the tunnel mainly passes through the highly weathered mudstone stratum. Mudstone is in brown grey, brown yellow, strong weathering, argillaceous structure, layered structure, joint fracture development, and the mineral composition is mainly clay minerals.

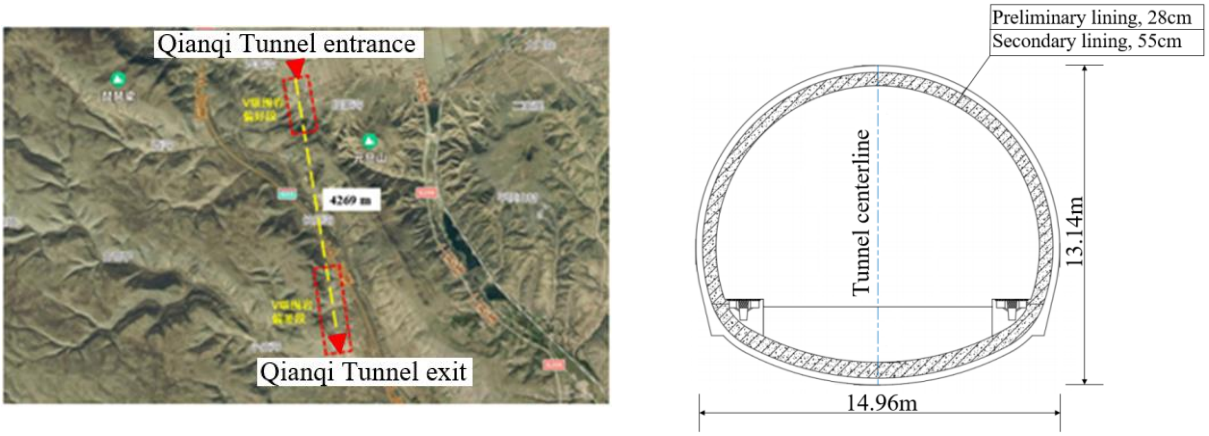

(a) Tunnel plan view *(b) Cross-section map*

Fig. 1 - Plan view and cross-section map of the Qianqi tunnel

NUMERICAL CALCULATION INSTRUCTIONS

Numerical model and calculation parameters

FLAC3D software is used to establish a numerical calculation model for the entrance (competent V-grade surrounding rock section, called condition I) and exit (poor V-grade surrounding rock section, called condition II) of Qianqi tunnel, as shown in Figure 2. As the buried depths of the entrance and exit of tunnel are similar, the buried depth is all taken as 28 m according to the site condition. To reduce the impact about boundary effect, the distance from the tunnel outline to the boundaries is generally taken more than 3 times the tunnel diameters. Therefore, the model size is: length × height × longitudinal length =150 m×110 m×30 m. Normal constraint is set to the front, back, left, right as well as bottom boundaries of the model, and the up boundary is a free surface [25, 26]. The rock and preliminary linings adopt solid element and shell element respectively, obeying Mohr-Coulomb yield criterions and elastic criterion respectively. The calculation parameter about rock as well as the lining is displayed in Table 1. Note that the calculation parameters are all taken from the on-site geological investigation and designed data.

Tab. 1 - Calculation parameter

Name	Density ρ /(kg.m^{-3})	Elastic modulus E /GPa	Poisson's ratio μ	Cohesion c /kPa	Internal friction angle φ/°
Condition I	2200	0.29	0.21	46	31
Condition II	1950	0.15	0.23	29	27
Preliminary lining	2300	34.9	0.2	-	-
Secondary lining	2500	31.5	0.2	-	-

The preliminary lining adopts C25 shotcrete, and the steel arch adopts I22a I-steel. The effect about the steel arch is transformed to the shotcrete by its elastic modulus. The calculation method [27] is as Equation (1):

$$E = E_0 + \frac{S_g E_g}{S_c} \tag{1}$$

Where: ***E*** refers to the elastic modulus about the concrete after conversion; E_0 refers to the elastic modulus about the original concrete; S_g refers to the cross-sectional area about the steel arch; E_g refers to the elastic modulus about the steel; S_c refers to the cross-sectional area about the concrete.

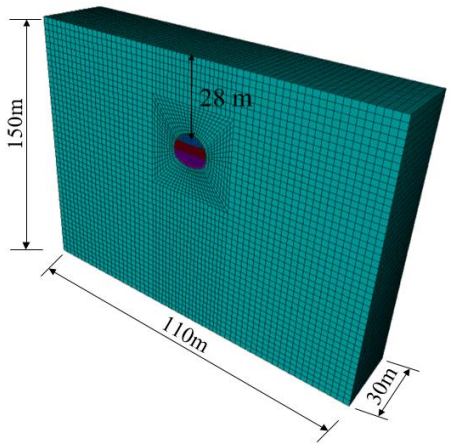

Fig. 2 - Calculation model

Calculation step

The tunnel construction method uses the three-bench excavation method, and the step length is generally 3~5 m ultra-short step. According to the on-site excavation footage (taken as 1.2m), the initial step shown in Figure 3 is excavated first, which is used as the basic model for the excavation footage studied in this paper. This paper mainly analyzes the deformation law as well as the mechanics about surrounding rock and preliminary linings under different excavation footage (1 m, 1.5 m, 2 m, 2.5 m, 3 m, 3.5 m), aiming to obtain the optimal excavation footage.

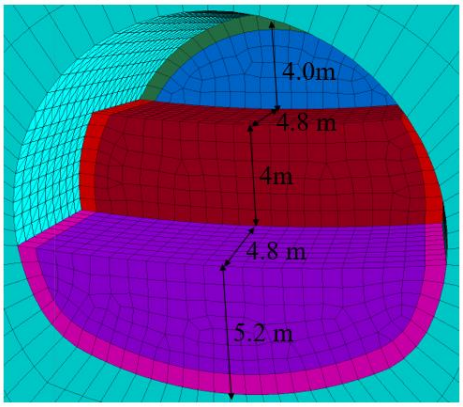

Fig. – 3 Initial step

The main calculation steps are as follows: (1) establish the calculation model; (2) ground

stress balance (only consider the self-weight stress); (3) partial excavation forms initial steps. First, the upper step is excavated at a depth of 1.2m, and the preliminary lining is applied with a lag of one footage. In the cycle of this excavation footage, the upper step is excavated to a depth of 9.6m, and then the middle step is similarly excavated cyclic to a depth of 4.8m, forming the basic model of excavation footage research in this paper; (4) excavate the tunnel according to the planned different footage.

ANALYSIS OF THE CALCULATION RESULTS

Deformation characteristics about the surrounding rock

Settlement characteristics of the vault

Under different excavation footages, the settlement and deformation about the surrounding rock at vault in front of the initial excavation face are shown in Figure 4. The zero of the horizontal coordinate corresponds to the initial excavation face of the upper step of the tunnel (called as the initial excavation face), that is, the longitudinal coordinate y= 9.6m, and the horizontal coordinate increases with the excavation direction of tunnel.

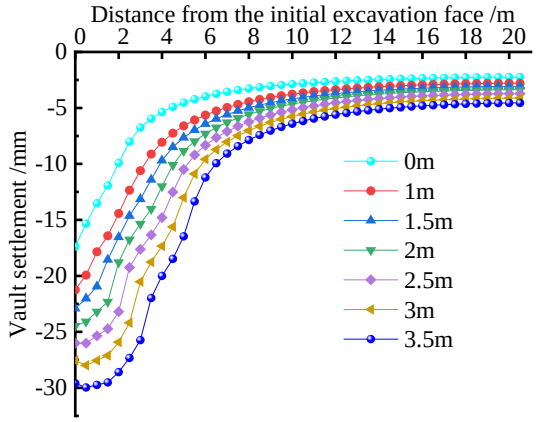

(a) Condition I

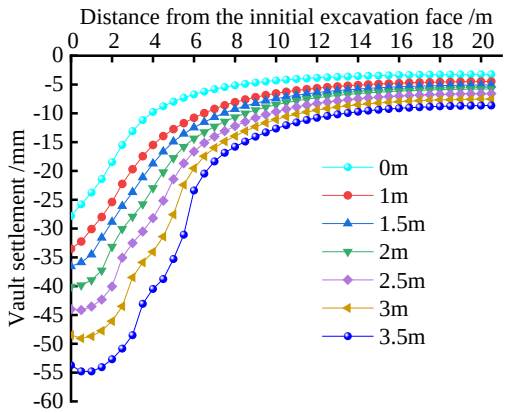

(a) Condition II

Fig. 4 - Distribution rule of the vault settlement under different excavation footages

In Figure 4, under conditions I and II, the law of the vault settlement is basically the same, all indicating that the larger the excavation footages, the larger the growth extent and influence range of settlement, and this law is nearly coincident with the previous literature [28]. Under 3.5m excavation footage, the maximum settlement is 1.95 times and 1.97 times of the initial settlement, respectively. And the larger the excavation footage, the longer the longitudinal range required for the settlement curve to decay to the stable state, that is, the larger the excavation footage, the wider the settlement influence range. Under different excavation footages, the increment of the maximum vault settlement caused by excavation of one cycle footage is relative to the initial step state. The fitting function curve and relation of the maximum increment of vault settlement with the excavation footages is shown in Figure 5. And the function is: $y=-3.4478x-17.681$ for condition I and $y=-1.0538x^2-3.305x-29.197$ for condition II.

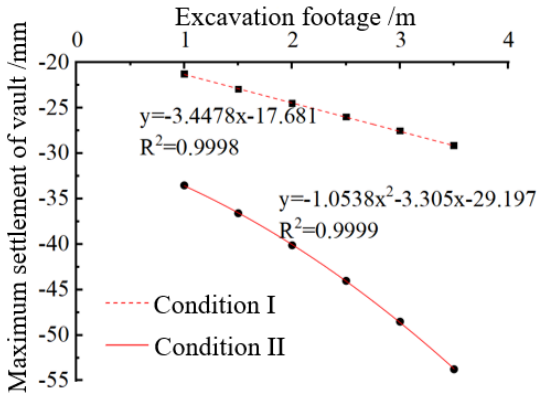

Fig. 5 - Fitting curve between the excavation footages and maximum vault settlement

To study the impact about various excavation footages on the vault settlement of the existing lining of the initial step, the monitoring points at vault in the middle of the vault of the initial step are selected as the investigation section, namely, middle step at y= 2.4m (Point A) and the upper step at y= 7.2m (Point B).

Figure 6 shows the curve of the vault settlement increment led by tunnel excavation in the middle step as well as the up step along with the excavation footages.

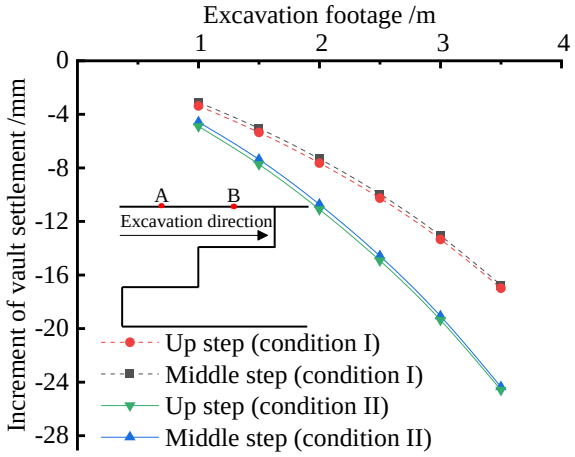

Fig. 6 - Curve diagram of the vault settlement increment and excavation footages at the monitoring points A and B

In Figure 6, under the same surrounding rock condition, the increment curves of the vault settlement of the middle step and the up step almost coincide. Therefore, it can be inferred that the initial settlement about vault above the step led by excavation is basically the same no matter how much the excavation footage is. The settlement increment about the vault of preliminary lining increases nonlinearly with the excavation footages, and the difference of the vault settlement increment in condition II is more obvious than that in condition I.

Horizontal deformation characteristic

The cloud image of horizontal displacement of rock under condition I with the excavation footage of 2 m is displayed in Figure 7. After tunnel excavation, the maximum horizontal deformation

of rock mainly occurs at the side wall of the newly-closed preliminary lining.

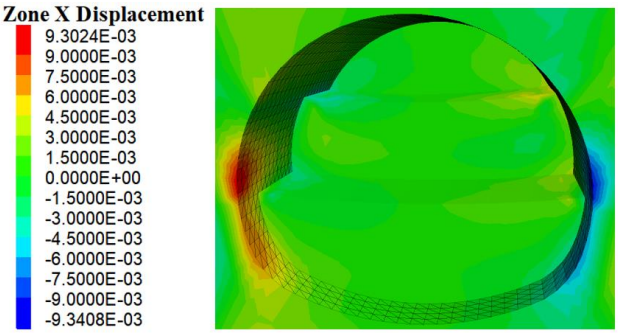

Fig. 7 - Horizontal displacement cloud nephogram of the surrounding rock in condition I /m

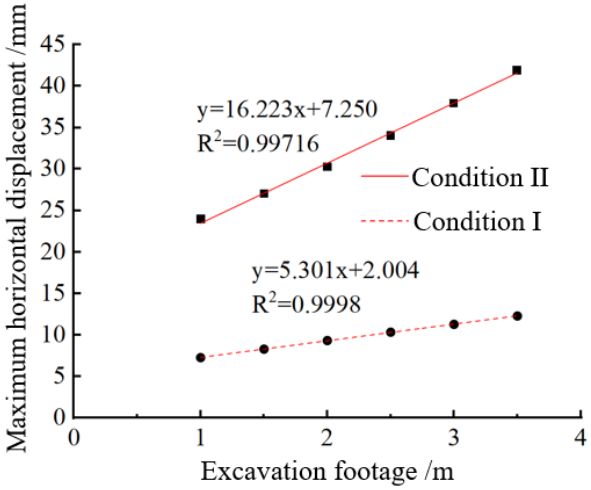

Fig. – 8 Fitting function curves of the maximum horizontal displacement and excavation footages in the excavated section

The fitting function curve of the largest horizontal displacements and excavation footages is displayed in Figure 8. There are good linear relationships between the largest horizontal displacements and excavation footages under the conditions I and II, and the specific fitting function relationship is as follows: y=5.301x+2.004 for condition I and y=-16.223x+7.250 for condition II.

The slope of the curve of condition II is much higher than that of the condition I. Therefore, the greater the excavation footages, the greater the maximum horizontal displacements about condition II. For the poor rock condition, the monitoring about the side wall of the newly-closed preliminary lining in each excavation cycle should be strengthened after construction.

Surface settlement law

The surface settlement curve of the section at longitudinal distance y= 9.6m under different excavation footages of conditions I and II is displayed in Figure 9. The influencing ranges about the settlement are nearly 60 m, and the largest settlement appears at the center line of tunnel. Under the adopted excavation footages ranging from 1 m to 3.5 m, the maximum surface settlement about the condition II is 2.02, 2.08, 2.16, 2.25, 2.35 and 2.47 times that of condition I, respectively. Similar to the spatial distribution of the vault settlement in front of the initial excavation face, that is, the larger the excavation footages, the larger the surface settlements as well as the growth rate.

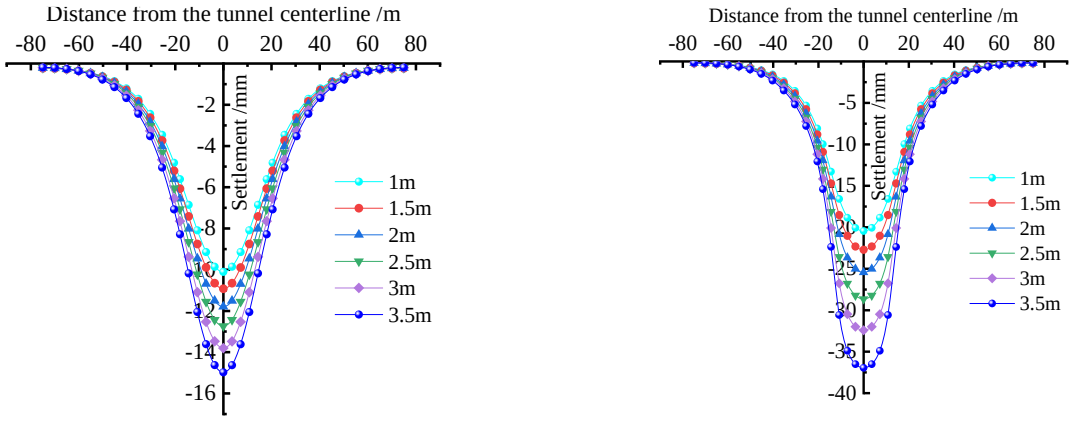

(a) Condition I (b) Condition II

Fig. 9 - Surface settlement curve under different excavation footages

Deformation characteristics of the excavation face

Figure 10 shows the on-site extrusion deformation phenomenon of the excavation face of tunnel. After exploration and analysis, the main reason is that groundwater develops in the rock in front of the excavation faces. Furthermore, highly weathered mudstone is a kind of rock that is more sensitive to water and is prone to strength softening and disintegration after encountering water, thus losing its bearing capacity.

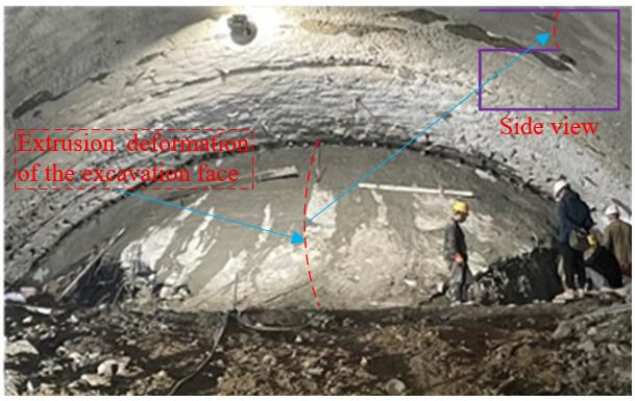

Fig. 10 - The on-site extrusion deformation phenomenon of the excavation face of tunnel

The fitting curves about the largest extrusion deformation of the up-step excavation faces and excavation footages under different rock conditions is displayed in Figure 11. Under these two surrounding rock conditions, the fitting function relationship between the maximum extrusion deformation of excavation face and excavation footages is as follows: $y=3.0857x^2-7.68x+51.309$ for condition I and $y=0.7143x^2-1.4886x+19.646$ for condition II.

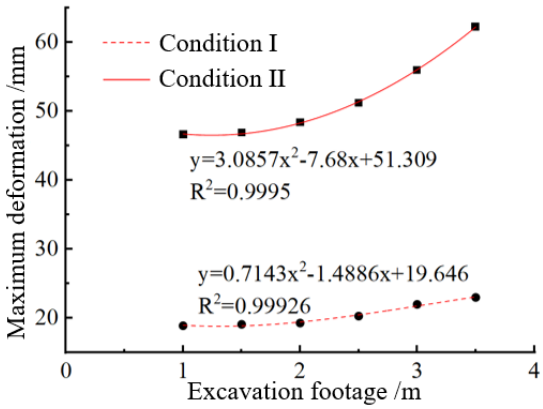

Fig. 11 - The function fitting relationship between the largest deformation about the excavation face and excavation footages

In Figure 11, under conditions I and II, the largest extrusion deformation about the excavation face and excavation footage show a significant quadratic function relationship. The maximum deformation about the excavation faces in condition II is much greater than that under condition I, so the strength of surrounding rock greatly influences the extrusion deformation characteristic of excavation face, and the maximum extrusion deformation increases nonlinearly with the excavation footages. Under condition I, the maximum extrusion deformations about the excavation faces increase little with the excavation footages. While under condition II, the maximum extrusion deformation increases slowly when the excavation footage is 1~2 m, and then the continuous increase of the footages will lead to a rapid increase of the extrusion deformation.

Mechanical characteristic analysis

Mechanical characteristic of the preliminary lining

The positions on the tunnel vault and both sides of the middle and upper steps are selected as the monitoring points, and the bending moment diagram of the preliminary lining at the longitudinal depth of 4 m under various excavation footages is also drawn, as shown in Figure 12.

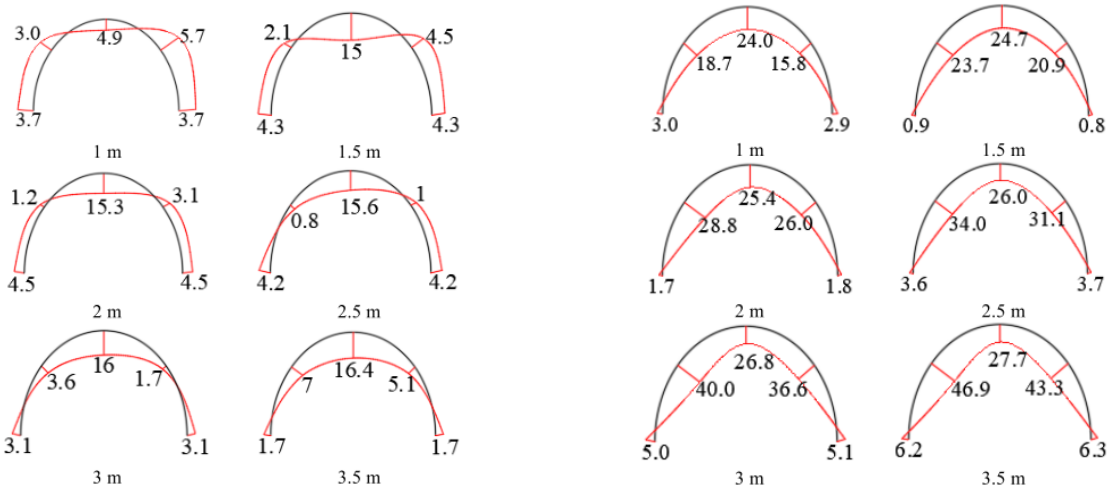

(a) Condition I (b) Condition II

Fig. 12 - Distribution of the bending moment of the preliminary lining under different excavation

footages /(KN.m)

Under condition I, the maximum bending moment generally appears at the vault of lining. The bending moment value about vault increases slowly when the excavation footage is more than 1.5m, the force state of the arch shoulder is gradually changed from the outer tensioned state to the inner tensioned state, and the inner tension range of the lining structure is gradually enlarged. Under condition II, the maximum bending moment is no longer located at the vault with the increase of excavation footages, but gradually shifts from the vault to arch shoulders. Bending moment at the arch shoulder increases more rapidly, while the bending moment at the vault increases slowly.

Mechanical characteristic of the surrounding rock

Figure 13 shows the distribution curves of the maximum principal stress (MPS) of surrounding rock at the vault as well as side wall about tunnel under different excavation footages in conditions I and II.

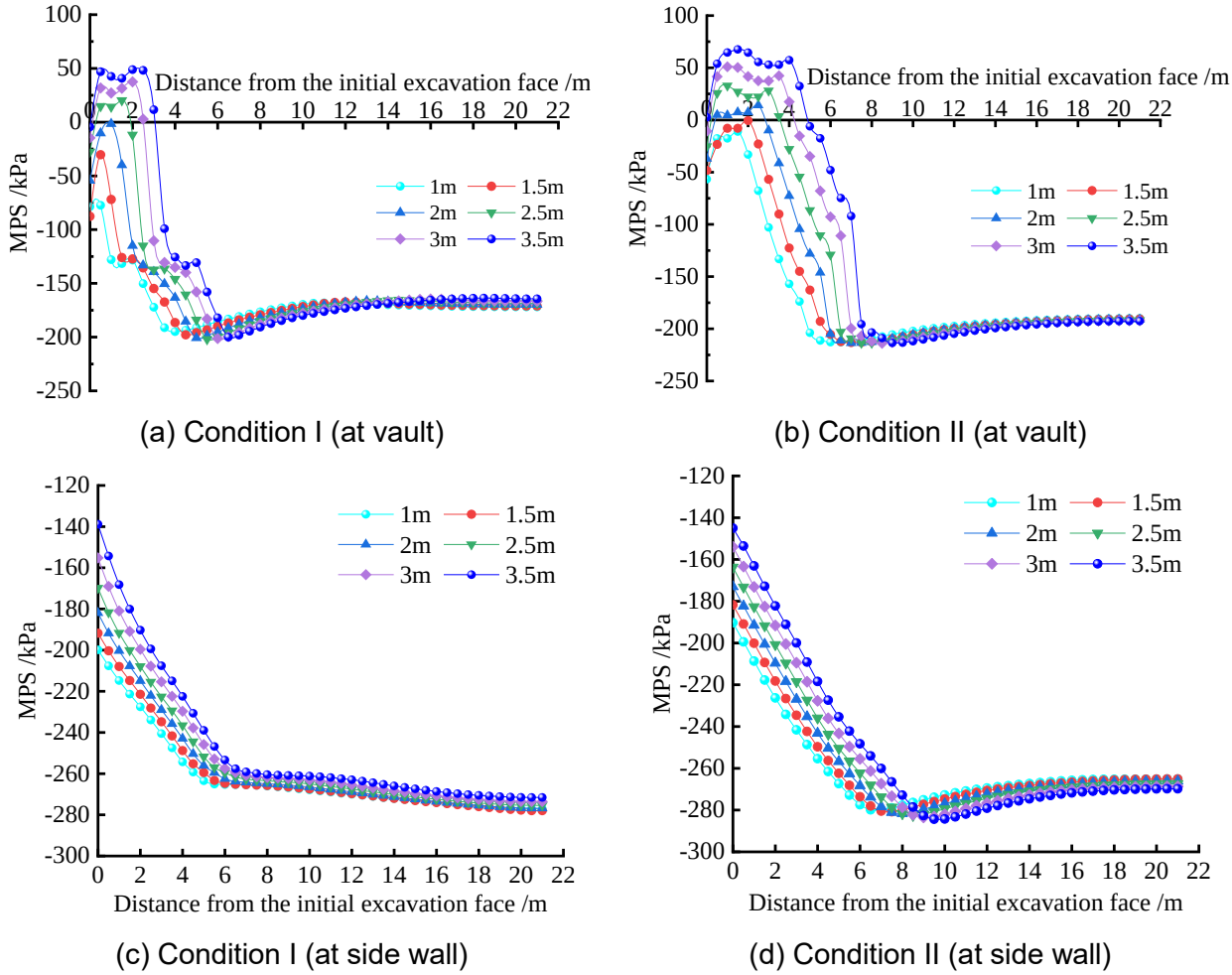

(a) Condition I (at vault)

(b) Condition II (at vault)

(c) Condition I (at side wall)

(d) Condition II (at side wall)

Fig. 13 - Mechanical characteristic curves of the surrounding rock under different excavation footages

In Figure 13, for both conditions I and II, the MPS curves show the law of first rapidly increasing, then rapidly decreasing, and finally stabilizing, and the rapid changes mainly occur near the excavation area. Under condition I, when the excavation footage is 1 m and 1.5 m, the peak MPS

of the surrounding rock is compressive stress. When the excavation footage reaches 2 m, the peak MPS of the vault of tunnel will be manifested as tensile stress, the main tensile stress and the action range of the vault gradually increases with the excavation footages. For the side wall, all of them are compressive stress, and the MPS is the minimum when the distances from the initial excavation face are zero. With the increase of distance from the initial excavation face, the MPS increases rapidly and then becomes stable. In general, under conditions I and II, it is still safer for the rock at the side wall of tunnel even if the excavation footage is larger.

According to Figure 13, the peak MPS corresponding to different excavation footages is extracted, and the fitting function curve between the peak MPS and excavation footages is drawn, as shown in Figure 14. The specific fitting relationship is as follows: $y=-3.0723x^3+23.884x^2-24.53x-7.3673$ for condition I and $y=5.0898x^3-50.345x^2+191.79x-223.41$ for condition II.

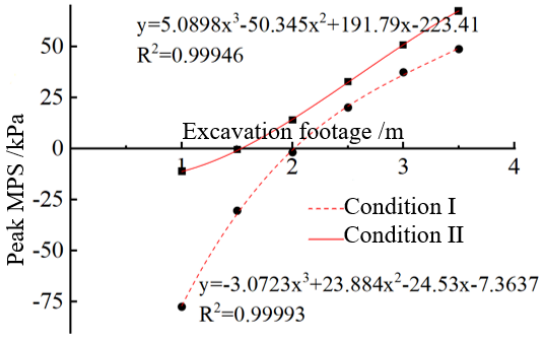

Fig. 14 - Fitting function curve of the peak MPS of the vault and excavation footages

Under condition I, for the excavation footages are more than 2 m, the tensile stress appears in the vault of surrounding rock. Under condition II, tensile stress occurs when the excavation footages are greater than 1.5m. In geotechnical engineering, it is generally believed that soil cannot withstand tensile stress, so the excavation footage under condition I should be less than 2 m, and the excavation footage under condition II should be less than 1.5 m. In order to ensure that no tensile stress occurs in the tunnel vault after excavation, the safety factor of 1.2 is adopted in this paper. Therefore, it is suggested that the excavation footage of the relied tunnel project of this paper should be 1.8m (for condition I) and 1.2m (for condition II).

CONCLUSION

(1) The deformation about V-grade surrounding rock is largely influenced by the excavation footages. The vault settlement and horizontal displacement of the tunnel as well as the surface settlement increase significantly with the excavation footages. Moreover, excavation in poor surrounding rock will not only lead to the increase of deformation, but also lead to the increase of the influence range of vault settlement.

(2) Under the competent or poor rock conditions, the maximum vault settlement in front of the initial excavation face, the maximum extrusion deformations about the excavation faces and excavation footages mainly show a positive correlation of quadratic function or linear relationship. The parameters of surrounding rock greatly influence the deformation about excavation face. For the lined steps behind the initial excavation face, the horizontal deformation of surrounding rock has

linear positive correlations with the excavation footages. Under the same surrounding rock condition, the vault settlement increment led by one excavation round is basically the same.

(3) For the competent surrounding rock, the maximum bending moments about preliminary lining at the middle step after excavation occurs in the vault, and the increase rate decreases when the excavation footage is more than 1.5m. For the poor rock condition, the maximum bending moment is transferred from the vault to the arch waist with the increase of excavation footages, and it is basically manifested as the inner tension of the lining. It is suggested that the optimal excavation footages about the relied tunnel project are 1.8m for the competent rock condition and 1.2m for the poor rock condition.

It should be noted that the comparison of the excavation methods and the influence of lining stiffness on tunnel in such soft rock are not considered in this paper, which can be further studied in the future.

COMPETING INTERESTS

The authors have no relevant financial or non-financial interests to disclose.

DATA AVAILABILITY

All data, models, and code used or used during the study appear in the submitted article.

REFERENCES

[1] Liu, J.G., Zhou, X.J., Xiao, Q.H., et al, 2017. Fault-related instability problems of tunnels - the host rock slip criterion and characteristics of the tunneling-induced shear displacements. Stavební Obzor - Civil Engineering Journal, Vol. 26, 441-458. https://doi.org/10.14311/CEJ.2017.04.0036

[2] Hou, F.J., Luo, Y.B., Jiang, Q., et al, 2020. Analysis on construction deformation and supporting structure of two-step and three section excavation method for super larger span highway tunnel. Stavební Obzor - Civil Engineering Journal, Vol.29, 110-123. https://doi.org/10.14311/CEJ.2020.01.0010

[3] Zhao, J.P., Tan, Z.S., Wang, X.Y., et al, 2022. Engineering characteristics of water-bearing weakly cemented sandstone and dewatering technology in tunnel excavation. Tunnelling and Underground Space Technology, Vol.121, 104316. https://doi.org/10.1016/j.tust.2021.104316

[4] Zhao, J.P., Tan, Z.S., Yu, R.S., et al, 2023. Mechanical responses of a shallow-buried super-large-section tunnel in weak surrounding rock: A case study in Guizhou. Tunnelling and Underground Space Technology, 131, 104850. https://doi.org/10.1016/j.tust.2022.104850

[5] Huang, J.Y., 2012. Parameters analysis and application of bench method for high-speed railway tunnels. Modern Tunnelling Technology, Vol.49, 77-82. https://doi.org/10.13807/j.cnki.mtt.2012.03.013

[6] Guan, B.S., 2016. Tunneling by mining method: lecture IX: methods for tunnel excavation and support. Tunnel Construction, Vol.36, 771-781. https://doi.org/10.3973/j.issn.1672-741X. 2016.07.001

[7] Wang, M.S., 2010. Tunnelling and underground engineering technology in China. China Communications Press, Beijing.

[8] Chen, L.B., 2008. Application of three bench method in reinforcing weak surrounding rock of railway mountain tunnel of passenger dedicated line. Journal of Railway Engineering Society, Vol. 25, 72-74.

[9] Sun, S.F., 2012. Construction technique for the Gujiping tunnel portal section in shallow-buried loess.

Modern Tunnelling Technology, Vol.49, 83-88. https://doi.org/10.13807/j.cnki.mtt.2012.04.017

[10] Liu, C., Peng, L.M., Lei, M.F., et al, 2019. Applicability & mechanical characteristics of shallow buried soft red clay tunnel under 3-step benching tunneling method with large arch feet. Journal of Railway Science and Engineering, Vol. 16, 2006-2017. https://doi.org/10.19713/j.cnki.43-1423/u.2019.08.018

[11] Zhang, X.L., 2012. Key factors affecting bench construction of a tunnel in soft rock. Modern Tunnelling Technology, Vol. 49, 60-62. https://doi.org/10.13807/j.cnki.mtt.2012.04.013

[12] Wang, Z.D., Gong, X.N., 2010. Calculation method of digging length in underpass with underground excavation under shallow cover. Rock and Soil Mechanics, Vol. 31, 2637-2642. https://doi.org/10.16285/j.rsm.2010.08.018

[13] Peng, X.J., Zhang, D.B., Yin, H.D., et al, 2022. Optimization of excavation footage of three-step method of shallow tunnels based on element safety coefficient method. Science Technology and Engineering, Vol. 22, 13973-13979.

[14] Li, H., Tian, X.X., Song, Z.P., et al, 2018. Study on calculation method of digging length for shallow tunnel based on Xie Jiajie's surrounding rock pressure formula. Journal of Xi'an University of Architecture and Technology, Vol. 50, 662-667. https://doi.org/10.15986/j.1006-7930.2018.05.007

[15] Jia, X.X., Zhao, Y.C., 2016. Analysis of mechanical behavior of tunneling in weak surrounding rock by CD method and benching method. Railway Standard Design, Vol. 60, 121-125. https://doi.org/10.13238/j.issn.1004-2954.2016.07.028

[16] An, Y.L., Ouyang, P.B., Yue, J., et al, 2019. Influence of excavation footage on shallow tunnel face stability and deformation and mechanics. Journal of Disaster Prevention and Mitigation Engineering, Vol. 39, 787-794. https://doi.org/10.13409/j.cnki.jdpme.2019.05.012

[17] Lu, X.G., Geng, J.Y., Pang, L., et al, 2022. Analysis of construction mechanical behavior and parameter optimization for subsequent tunnel tube of double-arch tunnel without middle drift. Modern Tunnelling Technology, Vol. 59, 80-90. https://doi.org/10.13807/j.cnki.mtt.2022.05.011

[18] Zhang, J.R., Wang, Z.Y., Feng, J.M., et al, 2021. Deformation control for large-section tunnel construction in fractured carbonaceous slate. Proceedings of the Institution of Civil Engineers: Geotechnical Engineering, Vol. 176, 132-145. https://doi.org/10.1680/jgeen.20.00212

[19] Zheng, C.C., He, P., Wang, G., et al, 2023. Simulation of bench stepping and optimization of bolt parameters based on multiple geological information fusion. Journal of Building Engineering, 79, 107941. https://doi.org/10.1016/j.jobe.2023.107941

[20] He, J.X., He, S.H., Liu, X.B., et al, 2023. Investigating the mechanical responses and construction optimization for shallow super-large span tunnels in weathered tuff stratum based on field monitoring and Flac3D modeling. International Journal of Civil Engineering, online. https://doi.org/10.1007/s40999-023-00891-9

[21] Zhou, Z.L., Zhao, J.P., Tan, Z.S., et al, 2021. Mechanical responses in the construction process of super-large cross-section tunnel: A case study of Gongbei tunnel. Tunnelling and Underground Space Technology, Vol. 115, 104044. https://doi.org/10.1016/j.tust.2021.104044

[22] Li, P.F., Zhao, Y., Zhou, X.J., 2016. Displacement characteristics of high-speed railway tunnel construction in loess ground by using multi-step excavation method. Tunnelling and Underground Space Technology, Vol. 51, 41-55. https://doi.org/10.1016/j.tust.2015.10.009

[23] Chen, Z.Y., Wang, Z.X., Su, G.S., et al, 2022. Construction technology of micro bench cut method for weak rock tunnel with high in-situ stress. Geotechnical and Geological Engineering, Vol. 40, 1407-1415. https://doi.org/10.1007/s10706-021-01971-0

[24] Shi, Y.Z., 2016. Evolution of ground settlement and support system behavior during benching excavation of a tunnel with super large cross section: A field monitoring case study. Electronic Journal of Geotechnical Engineering, Vol. 21, 4779-4798.

[25] Qiu, J.L., Fan, F.F., Zhang, C.P., et al, 2022. Response mechanism of metro tunnel structure under local collapse in loess strata. Environmental Earth Sciences, Vol. 81, 164. https://doi.org/10.1007/s12665-022-10256-5

[26] Zhang, H.J., Liu, G.N., Liu, W.X., et al, 2023. Analysis on the influence of dismantling temporary lining of closely-undercrossing subway. Geotechnical and Geological Engineering, Vol. 41, 3189-3202. https://doi.org/10.1007/s10706-023-02452-2

[27] Wu, B., Gao, B., Suo, X.M., et al, 2005. Mechanical simulation and analysis of construction behavior of urban metro tunnelling with small interval. China Journal of Highway and Transport, Vol. 18, 84-89. https://doi.org/10.19721/j.cnki.1001-7372.2005.03.019

[28] Yan, D.M., He, P., Chen, Z., et al, 2016. Research on excavation footage of tunnels in IV rock with two-bench construction method. Railway Standard Design, Vol. 60, 99-103. https://doi.org/10.13238/j.issn.1004-2954.2016.09.022